MPS Report: Photometry of Uranus' Rings*

Author: Kazem Ayat / PI: Prof. Imke de Pater/Advisor: Dr. Edward M. Molter†
Physics Department, University Of California: Berkeley
(Dated: August 12, 2023)

Abstract

This research investigates the nature of Uranus's ring system, with the primary goal of better understanding the surface roughness of the rings by measuring their change in brightness as a function of phase angle. There have been a lot of analyses on the rings of Uranus such as the Evolution of Dusty Rings (de Pater, 2006), Thermal Emission from the Uranian Ring System (Molter, 2019) and (Showalter, 2020), in which all unveil a new aspect of the rings. Such as general information on the rings' properties, thermal emissions of the rings, and I/F for some rings at some observation dates. No researcher has exclusively studied the brightness of the rings on many different dates (and in fact on selected desired dates) of observation as a function of phase angle. The study employed a method developed for interpreting calibrated K-band (2.1 microns) and H-band (1.6 microns) images from Hawaii's Keck Observatory, enabling the creation of radial profiles of Uranus's rings. The data was processed by implementing a masking technique, then applying the proper physical conversion. We used a fitting algorithm to determine the brightness of each of the inner main rings. This model was fit to data from August 2015, October 2019, and November 2019. The final product of this era is the tables in Fig.12 and Fig.13 where I have extracted the I/F on each date, on south or north ansa, on each band for 9 brightest rings. The research pushes the boundary of our understanding of Uranus's ring system, setting the stage for my future work aimed at obtaining standard,real I/F measures. As of July 26th, the research has yet to reach its final goal, implying a continuous progression toward further revelations about Uranus's ring system. Hence all the progress that has been achieved and recorded in this research is up to July 26.

I. INTRODUCTION TO URANUS' RINGS SYSTEM

The Uranus ring system has been one of the most interesting yet unknown aspects of our solar system. Studying the ring systems will eventually help us to understand many other interesting phenomena. We study these systems for three key reasons. First, they provide a wealth of information about the history and ongoing evolution of the planetary systems of which they are a part. Second, they are dynamical analogues for protoplanetary disks, exhibiting many of the same processes, but much easier for us to observe. Third, they have many mysterious and unexpected properties, which make them worthy of study in their own right; for example The Voyager 2 discoveries of Cordelia (inner-most moon of Uranus) provided dramatic support for the newly proposed 'shepherding' mechanism for ring confinement. Shepherding would allow each sharp ring edge to be maintained via torque balance with a nearby moon (Showalter 2020). Uranus has 13 different distinct rings with different properties. The inner system of nine rings consists mostly of narrow, dark grey rings. There are two outer rings: the innermost one is a dusty ring. In order of increasing distance from the planet, the rings are called Zeta, 6, 5, 4, Alpha, Beta, Eta, Gamma, Delta, Lambda, Epsilon, Nu, and Mu.Building upon the groundwork laid in previous research, which pioneered the study and observation of the thermal component of Uranus's ring system (Molter,2019), it is of critical importance that we continue to identify and accumulate detailed knowledge about these rings. The very final goal of this research is to understand the surface roughness of the rings better by measuring their change in brightness as a function of phase angle. This eventually will tell us essential physical properties of the ring particles, including surface roughness.

II. RADIAL PROFILE OF URANUS' RINGS

Prior to the summer of 2023, I developed a generic method to input any calibrated K-band or H-band images taken from the planet Uranus by Keck Observatory located in Hawaii (Fig.1).

The program can create a radial profile of the rings, which is the plot of the position from the center of Uranus vs. a non-standard measure of the flux (Fig.2).

* This report encapsulates all accomplishments up to July 26th 2023.
† All at University Of California:Berkeley.

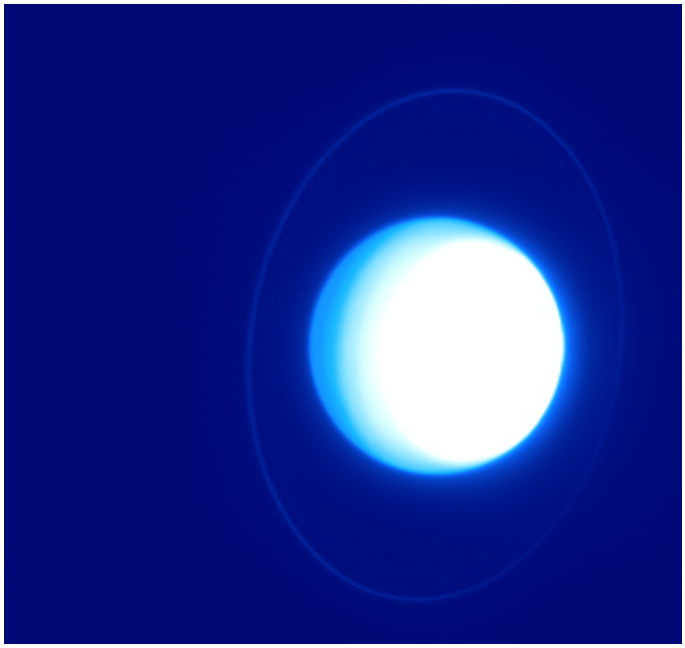

FIG. 1. A raw, calibrated image of the Uranus in H-band, taken from Keck Observatory (with an applied color map). Note the planet and the Epsilon ring. Other rings are too faint for eye to distinguish. That is a job suitable for computers to find out other rings in this image.

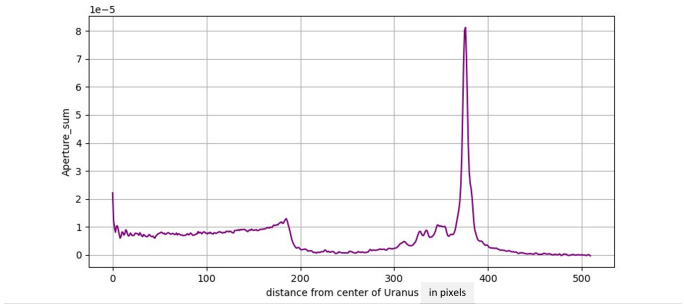

FIG. 2. The Radial profile of the Uranus' Rings. The artifact of the planet is visible from 0 to 240 pixels. The distinct peak is nothing but the brightest ring, Epsilon ring! Vertical is in an non-standard brightness unit which is valid for the sake of comparison

Most of the rings' artifacts are clearly visible and interpretable. The procedure is in fact, quite an interesting one! I developed an exact model of the Epsilon ring using an "Elliptical Annulus Object" with the aid of Python packages: pylanetary, astropy, photutils. So Rings could be modeled as an elliptical annulus. Once the ring's rotation angle, the inner and outer semi-major axis, the inner and outer semi-minor axis, and the apparent width of the ring were all set to that of the Epsilon ring, I took this structure and created the "smallest" possible concentric elliptical annulus similar to the epsilon ring, and successively with the steps of 1 pixel on the image I increased the length of minor and major axes. And created more annuli so it will contain all the rings on the image (Fig.3).

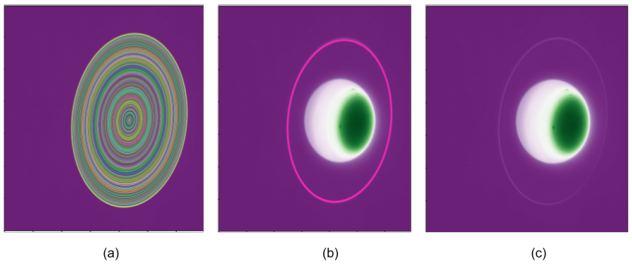

FIG. 3. How the Algorithm works: (a): Creating all the possible specified annuli (b): the specific annulus of interest which in this case is the Epsilon ring (c): The original data

III. MASKING THE DATA

Note that no matter the image's band (K or H) the light scattered from the planet is always considered a setback in acquiring data from the rings. Hence it would be wise to mask off the planet itself so the features of the rings get the chance to intensify. By determining the center of the planet, and setting the coordinates of two other points on the image I can mask any image (Fig.4). Note that we perform masking on each image and then use it to generate the radial profile and all other operations. It is stunning to compare how much the fitting helps to improve the data (i.e. radial profile). For example, consider the data taken on August 2015 (Fig.5). It is quite easy to qualitatively recognize the potential depth of the details that masking unlocks in our data. And thus masking is a necessity that must be applied to all the images before any processing or analysis.

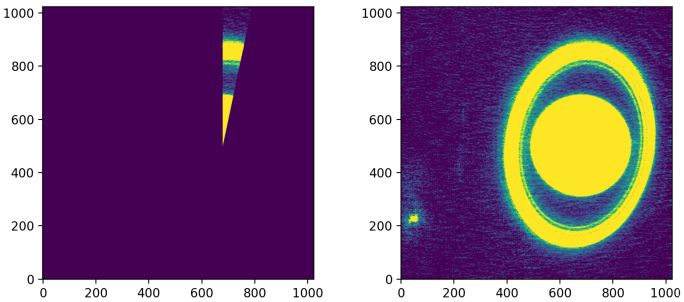

FIG. 4. A comparison of masked and unmasked images. Note that axis are in pixels. left is masked and right is unmasked original image (August 2015).

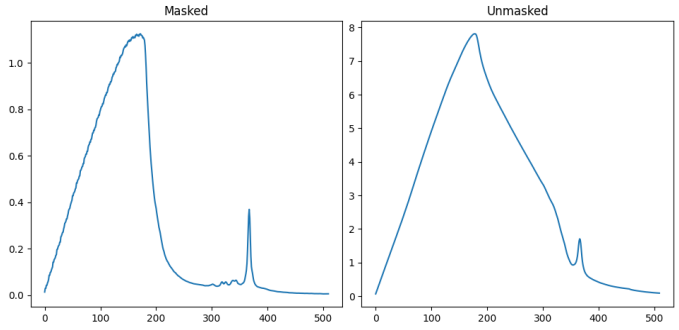

FIG. 5. A comparison of masked unmasked images on August 2015. Note the amount of details that masking unlocks. Vertical is in an non-standard relative brightness unit which is valid for the sake of comparison. Horizontal is in pixels. These are the results derived from Fig.4

IV. RING SYSTEM MODELING

Next, the analysis goes further and develops a model of the ring system. I have constructed a perfect resolution model which just ends-up being 9 Dirca-Delta functions representing the 9 mostly visible rings in my radial profile and then convolved them with the point-spread function-PSF- (more on this in the next sections) which is directly a property of the telescope. Now the goal was to fit this function into the actual radial profile. For the fitting procedure, I initially (prior to the summer of 2023) included 9 degrees of freedom each corresponding to the amplitude of the Dirac-Delta function. The fit clearly showed potential, but yet it was far from a worthy fit, and we encountered some discrepancies in matching our model to our fit. Hence recently I have included 3 more degrees of freedom in the fitting procedure. So now there is some room for the rings: Epsilon, Alpha, and Beta to move horizontally (a horizontal shift for each corresponding Dirac-Delta function). This ended up making my fit much better. Fig.6 with the residual plot demonstrates how good our fit is.

Note that since there is no such thing as a perfect Dirac-Delta function in real life, I have interpolated the data with a very large interpolation axis (to account for the sanity of an ideal Dirac Delta function). Note that I have reduced the light scattering from the planet (which is a major setback in rings' detection) on all the H-band images (due to the nature of the H-band), and then used them to perform the modeling procedure. More on this and its procedure in the next sections. Note that I have applied all these modeling procedures to 3 K-band data and 3 H-Band data taken on August/2015, Oct/2019, Nov/2019. For each image, I have also masked the "top/northern" and "down/southern" ansa. Since processing each ansa region will equally yield useful information. So a total of 12 images/data must be processed with my current data.

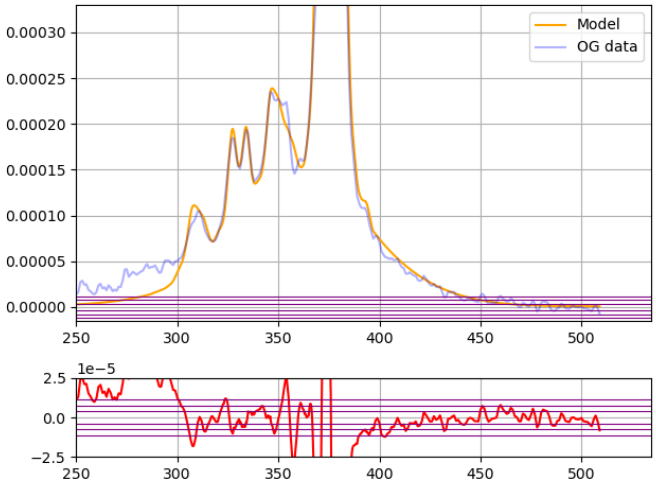

FIG. 6. A plot that demonstrate the my fit on the radial profiles and the residuals. Vertical is in fact in the unit of I/F per pixel, and horizontal is in pixels. the fit looks reasonable, but is there room for more improvement? Data: Oct 2019, North ansa, K-band

V. CREATING AND SMOOTHING OUT THE PSF (POINT-SPREAD FUNCTION)

I used the general technique outlined in (2006, de Pater). In order to generate the point spread function, I used the right side of the Epsilon ring in the radial profile (the highest peak in Fig.2). But this function was too noisy, so I smoothed out the wing of the PSF (and not the peak of the PSF to conserve the "sharpness" of the plot) using a boxcar averaging with the Kernel width of 80. Once this was smoothed, I fitted this curve with a 4th-degree polynomial (with 4 degrees of freedom), and then used the 4th-degree polynomial fit as my right half of the PSF. In order to complete the PSF I mirrored the PSF and developed the left side of the PSF. The final function acts as my PSF throughout the whole process. (Fig.7).

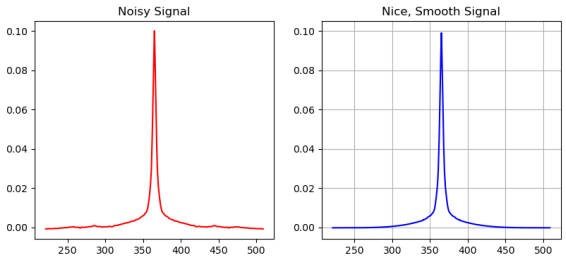

FIG. 7. A comparison of PSF before and after smoothing it out. horizontal is in pixels.Vertical is in an non-standard brightness unit which is valid for the sake of relative comparison.

VI. REMOVING THE LIGHT SCATTERING OF THE PLANET ON H-BAND IMAGES

The nature of the H-band images makes it necessary to reduce the light scattered from the planet. Since these lights influence the visibility of the ring data (they are so bright on the H band). In order to do that I have considered that the light scattered from the planet could be modeled as the legs of a Gaussian function. Hence after this modeling/fitting (Fig.8), and subtracting the fit from the original radial profile on the H-band, we end up with a similar plot to (Fig.2) which was that of a K-band image. And this grants that we can use the H-band images in our modeling procedure just as well as K-band images.

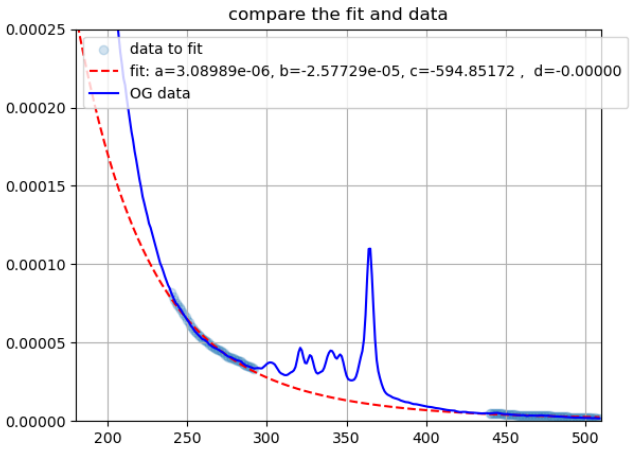

FIG. 8. Comparing the fit and data. Horizontal is in pixels,Vertical is in an non-standard brightness unit which is valid for the sake of comparison.

VII. METHODS AND TECHNIQUES IN UNIT CONVERSION TO I/F

Imagine that we have not masked our data. Then in order to convert my y-axis data to meaningful quantities, I just have to divide the acquired initial value of the rings' photometry (and all images are calibrated) by the whole area of each corresponding elliptical annulus. That would be easy. The reason is that there are already premade tools and programs to calculate this area (Photutils package). But with the masking procedure, I should not divide by the area of the corresponding elliptical annulus, but I should divide by the area of the corresponding elliptical annulus sector! This was a mathematical complexity that must be addressed properly. Using parameterization in polar coordinates and integrating from two different angles, it is easy for one to derive the equation of the area of the sector of an ellipse with its semi-major axis aligned on the x-axis (Fig9, and Fig.10).

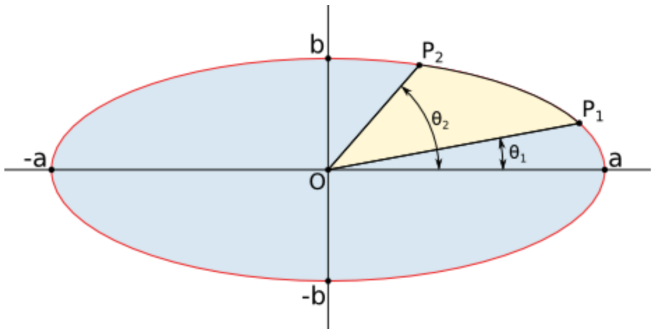

FIG. 9. The correct coordinate and the graphical setup of the process for finding the area of the elliptical sector.

$$\frac{1}{2}ab\left(\tan^{-1}\left(\frac{a\tan(\theta_2)}{b}\right)-\tan^{-1}\left(\frac{a\tan(\theta_1)}{b}\right)\right)$$

FIG. 10. This is the relation that governs the area of the elliptical sector based on the two so called angles (see Fig.9) and semi minor and major axis.

Now by subtraction of the area of the sector of the outer ellipse from the area of the sector of the inner concentric ellipse, I can get the area of the sector of the elliptical annulus. There was still one complication that I should have taken care of before the sector areas calculation. Note that the condition for our derivation requires to have the semi-major axis (a) overlap my x-axis of the coordinate system. So this fact boils down to a coordinate transformation. In order to meet this condition there must happen a coordinate transformation in this order:

1. a translation of the origins from the old origin (0,0) to the new origin which is the center of the planet.

2. a rotation equal to the magnitude of the rotation angle of the rings! This angel is an attribute of the Epsilon ring per se and it is accessible from the earlier codes on the radial profile section.

A graphical overview of how this coordinate transformation should happen is outlined in (Fig.11).

It is worth to note if I am using a northern ansa for data analysis a positive value for the rotation angle must be used. If it is a southern ansa, the same angle must be used but with a negative sign. So once the coordinate on the image is completely transformed the areas can be acquired. And then I divided them by the acquired initial aperture sum to get the new more sensible quantity "I/F per pixel". Note that I/F is simply a measure of comparing the intensity and flux of the light source, which is very common to use among astronomers. But note that this is the acquired value is "I/F per pixel". In order to

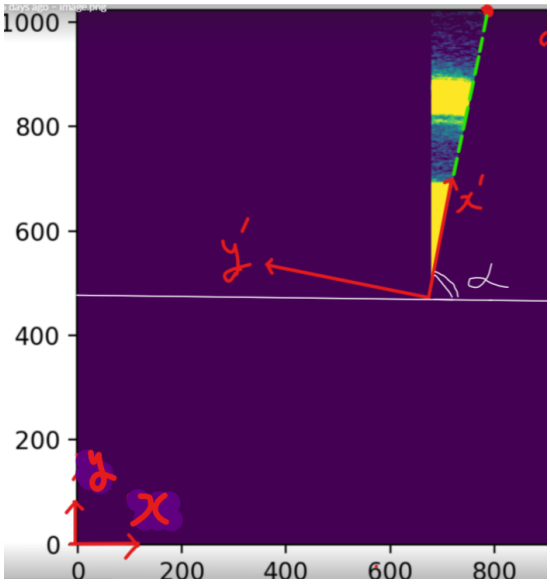

FIG. 11. This figure outlines graphically how the coordinate transformation must happen. Units are all in pixels. We want to transform from the xy system to x'y' system

obtain the real I/F I still have works to do. So far the research reaches this limit. It is the reach of this research. End of documentation until July 26th 2023.

VIII. CONCLUSION

In this research, an exploration of Uranus's ring system was undertaken, with the main goal being to understand the surface roughness of the rings by examining their brightness as a function of phase angle. Utilizing the Keck Observatory's calibrated K-band and H-band images, radial profiles of Uranus's rings were generated, and the brightness of the inner main rings was determined through the implementation of a fitting algorithm. The resultant tables, presented in Fig.12 and Fig.13, provide insight into the relative brightness of the rings. This study promises advancement in the field, it will provide valuable information on the surface roughness of the rings. As the research is progressing toward its ultimate goal. The future steps will be to obtain the actual flux for each ring. Right now what we have in the tables is I/F for only a segment of the ring (a slice due to masking). We need to obtain that for the rings completely. This is an easy task for all the rings except the Epsilon ring. Since the brightness is not uniform throughout the Epsilon ring. Hence we need to look at the azimuthal ring profile to extract the flux for the Epsilon ring from there. Note, that this would be only applicable for K-bands, for H-band (because of the light scattered by the planet) we have to only use the 2 ansae points (the trusted points for I/F) and use a multiplicative conversion factor to convert the K-band flux to meaningful H-band I/F since they have captured on the same time. I am also developing an updated version of my masking mechanism. This updated version works based on the location of the rings' ancae, and it provides a more systematic and scientific scheme for our analysis. All in one, we still got a bit of work to do, but we are almost there, and can get to this soon! Thanks for reading!

IX. REFERENCES

de Pater, Imke, 2006, Evolution of Dusty Ring,[1]

Molter , Edward, 2019, Thermal Emission from the Uranian Ring System [2]

Showalter , Mark, 2020, The rings and small moons of Uranus and Neptune [3]

```
==========================================   K-Band       ============================================================================

koct2019N.npy
eps        del        gam        eth        bet        alp        fou        fiv        six
0.0018208  0.0000608  0.0000841  0.0001238  0.0001113  0.0001254  0.0000313  0.0000340  0.0000584
koct2019S.npy
eps        del        gam        eth        bet        alp        fou        fiv        six
0.0015635  0.0000725  0.0001185  0.0001438  0.0001205  0.0001671  0.0000216  0.0000214  0.0000902
knov2019N.npy
eps        del        gam        eth        bet        alp        fou        fiv        six
0.0019378  0.0000720  0.0001061  0.0001698  0.0001179  0.0001443  0.0000367  0.0000373  0.0000694
knov2019S.npy
eps        del        gam        eth        bet        alp        fou        fiv        six
0.0018696  0.0000989  0.0001458  0.0001553  0.0001162  0.0001791  0.0000381  0.0000482  0.0000850
kaug2015N.npy
eps        del        gam        eth        bet        alp        fou        fiv        six
0.0018694  0.0000662  0.0000873  0.0001358  0.0001340  0.0001364  0.0000382  0.0000363  0.0000695
kaug2015S.npy
eps        del        gam        eth        bet        alp        fou        fiv        six
0.0010755  0.0001647  0.0001253  0.0002559  0.0001952  0.0002559  0.0000622  0.0000013  0.0001325
```

FIG. 12. Table of relative brightness of each ring and dates in K-band in unit of I/F per pixel. Naming Convention: "koct2019N" which is "band-month-year-SouthOrNorth", and for rings, I used the first three characters in their name.

```
==========================================   H-Band       ============================================================================

hoct2019N.npy
eps        del        gam        eth        bet        alp        fou        fiv        six
0.0015963  0.0000437  0.0000944  0.0001594  0.0000770  0.0001289  0.0000215  0.0000274  0.0000441
hoct2019S.npy
eps        del        gam        eth        bet        alp        fou        fiv        six
0.0013457  0.0000872  0.0001222  0.0001078  0.0001072  0.0001332  0.0000206  0.0000379  0.0000281
hnov2019N.npy
eps        del        gam        eth        bet        alp        fou        fiv        six
0.0015137  0.0000445  0.0000941  0.0001554  0.0000866  0.0001059  0.0000143  0.0000204  0.0000375
hnov2019S.npy
eps        del        gam        eth        bet        alp        fou        fiv        six
0.0013295  0.0000897  0.0001140  0.0001292  0.0001095  0.0001380  0.0000170  0.0000405  0.0000283
haug2015N.npy
eps        del        gam        eth        bet        alp        fou        fiv        six
0.0016034  0.0000361  0.0000652  0.0001199  0.0000947  0.0001115  0.0000160  0.0000227  0.0000350
haug2015S.npy
eps        del        gam        eth        bet        alp        fou        fiv        six
0.0008807  0.0001262  0.0000977  0.0001413  0.0001241  0.0001600  0.0000122  0.0000378  0.0000209
```

FIG. 13. Table of relative brightness of each ring and dates in H-band in unit of I/F per pixel. Naming Convention: "hoct2019N" which is "band-month-year-SouthOrNorth", and for rings, I used the first three characters in their name.